Convertible Sketches of Mechanical Curved Objects into 3D Models

Masaji Tanaka[1], Rikuu Zenkai[2], Weiqiang Liu[3], Chiharu Higashino[4] and Masaaki Ohtsuki[4]

[1]Okayama University of Science, masaji-tanaka@ous.ac.jp
[2]Mebius Packaging Corporation, rikuu_zenkai@mebius-pkg.co.jp
[3]AKTIO Corporation, dfjzxxspp@gmail.com
[4]Aikoku Alpha Corporation, {higashino, ohtsuki}@aikoku.com

Corresponding author: Masaji Tanaka, masaji-tanaka@ous.ac.jp

Abstract. Sketches in the form of line drawings are important for designers to express overviews of objects, particularly mechanical objects, directly. Numerous methods have been proposed for the automatic conversion of sketches into 3D models. However, no practical conversion systems have been developed thus far. We developed a *sketch feature-based conversion method* (SFBCM) for this purpose. In SFBCM, when a sketch is input, *sketch features* (SFs), which are simple sketches of objects such as cubes and cylinders, are detected and extracted as 3D features step-by-step from the sketch, whereby these are combined in accordance with the sketch to obtain a 3D model. For more complex sketches, *abstract sketch features* (ASFs) are introduced into SFBCM to predict the hidden shapes of the sketches. *Accessorial sketch features* (ACSFs) are introduced to handle the sketches of chains, springs, and screws, which are important mechanical parts with unique symbolic expressions. Through these studies, we clarify the entire image of convertible sketches for mechanical curved objects. In this paper, the limitations of the sketches, including the curves for the conversion, are clearly described, and several new curved SFs are introduced. Finally, the effectiveness of the updated SFBCM is demonstrated using several advanced examples.

Keywords: Convertible sketch, Mechanical curved object, SFBCM, 3D Model.
DOI: https://doi.org/10.14733/cadaps.2025.400-413

1 INTRODUCTION

Sketches in the form of line drawings are commonly observed in magazines, books, and manuals, among others. Sketches are also important for designers, particularly mechanical designers when inventing new ideas for products and their parts. *Sketch-based modeling* (SBM) [14], specifically, automatic conversion of sketches into 3D models, is advantageous for a variety of applications, including computer-aided design (CAD), computer graphics (CG), and computer vision. For example, in the future, robots will be expected to understand sketches using converted 3D models. Over the

past 50 years, numerous methods have been developed to automatically convert sketches into three-dimensional (3D) models. However, no conversion system has been developed to date. We have been developing methods for converting sketches into 3D models for approximately ten years and have proposed a *sketch feature-based conversion method* (SFBCM) to achieve this conversion [18-23]. In SFBCM, each sketch consists of straight lines, ellipses, elliptical arcs, and sometimes Bezier curves, correctly drawn using 2D CAD systems as in the examples presented in this study. Each sketch is an orthogonal projection of an opaque object viewed from a general perspective.

A simplified explanation of SFBCM follows. Fig. 1 shows three basic *sketch features* (SFs): a cuboid, cylinder, and round hole. For example, a cuboid sketch can be defined as three parallelograms sharing three straight lines forming a *Y*-junction, as explained below. In SFBCM, when a sketch is input, a 3D model is obtained by detecting and extracting SFs as 3D features step-by-step and then combining them in accordance with the sketch. Fig. 2(a) shows Example 1, which is a sketch of the mechanical part. When this example is input into the SFBCM, first, a sketch of a cylinder (colored red) is detected, and its hidden lines can be drawn, as shown in Fig. 2(b). This step can be changed to the detection of a round hole, as shown in Fig. 2(c). The SF detection sequence is discussed later. Subsequently, the sketch of a cylinder is extracted as a 3D feature from this figure. After this extraction, although the two lines are broken, they are automatically restored by extending them. Fig. 2(c) shows the restoration and detection of a round hole sketch. No SFs are detected after hole extraction. In this case, additional lines are drawn to help detect SFs in SFBCM. Two additional lines can be drawn, such as the extended lines from the *W*-junctions- and *L*-junctions, as described below. Each extension continues until it intersects another line in a sketch; otherwise, it is removed. In Fig. 2(d), two additional lines are drawn from the *W*-junction. Consequently, a cuboid sketch is detected, as shown in Fig. 2(e). Although another additional line can create another cuboid sketch, this problem concerns the sequence of detecting SFs described above; therefore, this case is omitted for a simpler explanation in this example. After an SF is detected, additional useless lines are removed. Next, another cuboid sketch is detected, as shown in Fig. 2(f). Fig. 2(g) shows the main dimensions of Example 1. These dimensions are measured from the cubic corners (explained later), corresponding to the *Y*-junctions of the cuboid sketches. In SFBCM, we assume that sketches drawn by people are as isometric and symmetric as possible [20]. Therefore, the ratio of the lengths of the line segments in the sketch corresponds to the ratio of the lengths of the edges in the 3D model. Based on this assumption, all the 3D features can be modeled and combined, as shown in Fig. 2(a). Consequently, the solution to Example 1 can be obtained, as shown in Fig. 2(h).

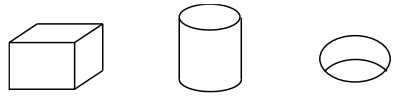

(a) (b) (c)

Figure 1: Three basic SFs: (a) Cuboid, (b) Cylinder, and (c) Round hole.

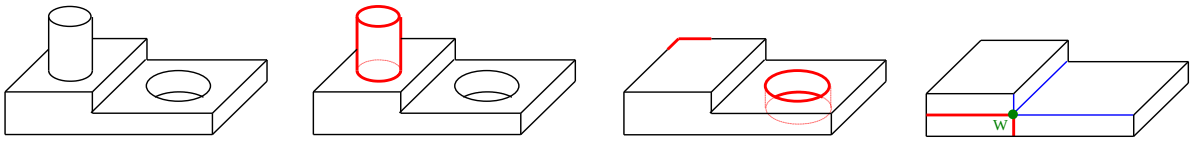

(a) (b) (c) (d)

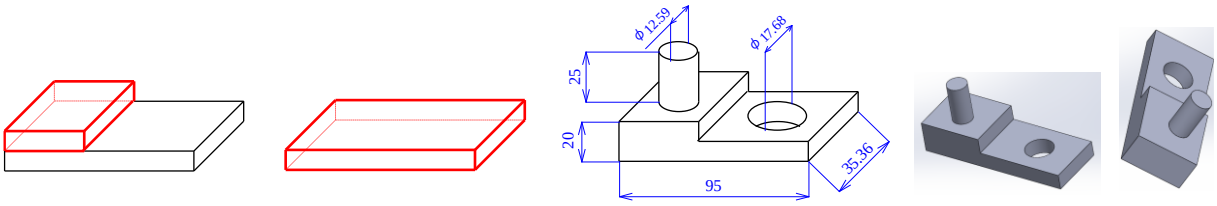

(e) (f) (g) (h)

Figure 2: (a) Example 1, (b) Detection of a cylinder sketch, (c) Restored corner and the detection of a round hole sketch, (d) Two additional lines from a *W*-junction, (e) Detection of a cuboid sketch, (f) Detection of the other cuboid sketch, (g) Main dimensions for modeling and combining 3D features, and (g) Two overviews of the solution.

We developed a method for predicting hidden parts in sketches using *abstract sketch features* (ASFs) [19], as explained later, introducing *accessorial sketch features* (ACSFs) for handling the sketches of chains, screws, and springs [18]. The main advantage of SFBCM is that it can handle sketches of polyhedral objects and curved objects such as cylinders and round holes. Although handling more complex curved objects seems difficult, the development of ACSFs suggests limiting convertible sketches to mechanical curved objects. Originally, we developed ACSFs for handling complex but important machine elements, such as chains, because the sketches targeted in SFBCM are primarily mechanical objects. Typically, a chain consists of several rings. However, if a ring sketch is defined as an SF, it becomes two ellipses, as shown in Fig. 3(a), making it difficult to recognize as a ring because the figure can be seen as a plate, as shown in Fig. 3(b). Therefore, we define a chain sketch as an SF, as shown in Fig. 3(c), and the rings making up the chain are defined as ACSFs. From this figure, two types of ACSFs are defined for the rings, as shown in Fig. 3(d). Many *T*-junctions (blue points) correspond to the intersections of two or three rings. Similarly, the sketch of the balls becomes a circle; therefore, it cannot be defined as an SF. This complicates defining curved objects with few edges as SFs. Therefore, SFBCM is not applicable to sketches of objects that are almost entirely composed of curved faces such as computer mice because they cannot be divided into SFs. This result corresponds to the difficulty of human perception in recognizing a computer mouse sketch as an accurate 3D model. Although handling sketches of mechanical as well as numerous other objects is desirable, this would require additional techniques, such as machine learning, as we attempted in [22] for SFBCM. According to the above theory, the convertible sketches of mechanical curved objects are limited in SFBCM, and this limitation accurately reflects human perception. Consequently, the purpose of this study is to address this limitation, by identifying several new curved SFs. The effectiveness of the updated SFBCM is illustrated by three advanced examples. The remainder of this paper is organized as follows: Related studies are discussed in Section 2. In Section 3 and 4, limitations and new SFs are described. In Section 5, the updated algorithm of SFBCM is explained with an example. Section 6 presents advanced examples. In Sections 7 and 8, several issues are discussed, and the conclusion is presented.

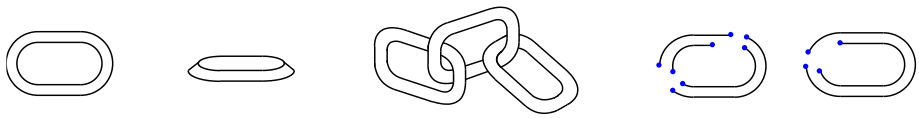

(a) (b) (c) (d)

Figure 3: Development of ACSF in a chain: (a) Ring sketch, (b) Plate sketch, (c) Chain sketch, and (d) Two types of ACSFs in rings.

2 RELATED WORKS

Studies concerning the conversion of sketches into 3D models have been surveyed in [4],[7]. Most studies are based on the Huffman-Clowes line labeling technique [6],[9]. In this technique, the objects in the sketches are limited to opaque trihedral polyhedrons, and the sketch is an orthogonal projection of an object viewed from a general position. Each line segment of a sketch is labeled as "+" (convex line), "-" (concave line), or with an arrow (occluding line). Based on labeling, all junctions of the lines are classified into four types: *L*, *W*, *T*, and *Y*-junctions. This naming was derived from the shapes of the alphabet, i.e., "L," "W," "T," and "Y," respectively. The relationships between the labeling and the junctions are summarized in a junction dictionary. Each junction represents a convex or concave shape of a 3D object drawn in a sketch. For example, if a *Y*-junction consists of three "+" lines, it expresses a convex shape. Kirousis [11] claimed that in a realizable sketch, all lines are uniquely labelable. Malik [12] extended this technique to include curved sketches, considering not only elliptical arcs but also free-form curves in the sketches. To the best of our knowledge, he was the only person who seriously addressed free-form curves in sketches. Therefore, our study is closely related to his, as described below:

A sample of line labeling is illustrated in Example 2, as shown in Fig. 4(a). In Fig. 4(b), each line segment is labeled. Arrowed lines (blue) indicate occluding edges. The twin-arrowed line (light blue) represents the limb line of the cylindrical face; "+" lines (red) express convex edges; "-" line (green) expresses a concave edge. From this figure, each junction can be recognized using a junction dictionary, as shown in Fig. 4 (c). The two red points represent *Y*-junctions. The right one expresses a convex corner because it consists of three "+" lines. The second is a concave corner. The four green, four blue, and three brown points represent the *W*, *L*, and *T*-junctions, respectively. These junctions were derived from Huffman-Clowes labeling. The following junctions were derived from Malik [12]. The four light blue *L*-junctions express *Curvature-L-junction*s, each consisting of a straight and a curved line. A gray *T*-junction expresses a *Three-Tangent junction* where a limb line is tangent to a "+"curved line and a curved arrow line. Each of the two pink points expresses a *Phantom-node* where a "+" curved and an arrow line form an ellipse. Although line labelling is not necessary in SFBCM, many junctions have been used to detect SFs, as in Example 1.

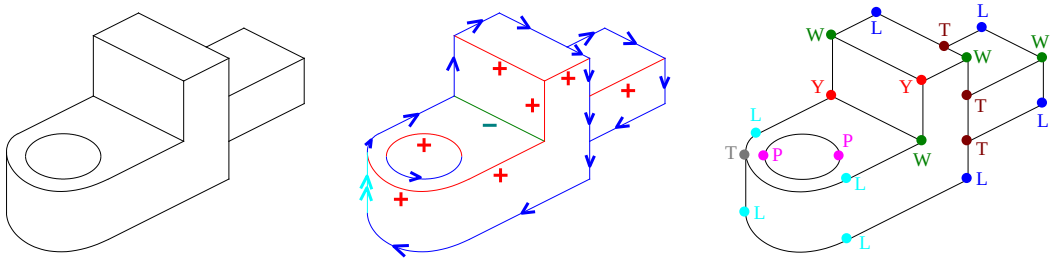

(a) (b) (c)

Figure 4: (a) Example 2, (b) Line labelling, and (c) Junctions.

Varley et al. [24] described a cubic corner based on [13] from a convex *Y*-junction. When a *Y*-junction is in an *x*-*y* coordinate system, and the three lines form a cubic corner, the equation can calculate all *z* values of the terminals in these lines. Consequently, *Y*-junctions expressing cubic corners in sketches can be precisely converted into 3D cubic corners. However, the results of the equation often do not fit the human perception. For example, a person can recognize a cuboid in Fig. 2(f) even though there are no rectangles in the cuboid sketches. Therefore, SFBCM regards this figure as a cuboid sketch using the human perception described in Example 1.

From a historical perspective, Biederman's geons [2-3], a modest set of generalized cone components, resemble SFs in terms of interpreting sketches as consisting of simpler sketches. However, SFs do not form a modest set of components for sketch representation but form a set of

simpler sketches convertible into 3D models. In addition, when looking at a sketch, the formation of geons can be related to the analysis and integration of human perception, whereas SFs can be regarded as the engineering elements of sketches for converting into 3D models. Therefore, they differ in the purpose of handling sketches, even if some hints are provided by geons to summarize SFs. In addition, Suh's algorithm [16-17] can be considered a pioneering work for SFBCM because it can convert sketches into 3D models using polygonal swept volumes, albeit with only few applicable sketches.

On the other hand, neural network techniques, particularly deep learning techniques, have been actively used for this conversion. In particular, the development of a single-image depth estimation technique for scene understanding [5],[15], has been applied to automatically reconstruct the 3D shape of an object from a single depth image [1],[25]. These techniques are effective for known objects such as tables, chairs, and couches because they are based on image processing. However, precisely and geometrically converting a sketch of a mechanical object, particularly a creative object, into a 3D model using these techniques is difficult. In addition, when performing SFBCM, one of the preconditions is that the sketch be a general view of an object. Therefore, as long as the sketch meets this precondition, it does not matter whether the object is a chair, table, or something else, even though learning techniques require massive amounts of data for each object category.

In summary, although all the studies described above are effective for conversion, converting sketches into 3D models is simpler and their limitations have not been clarified. This study aims to clarify this limitation for mechanical curved objects and presents advanced examples.

3 LIMITATION OF CONVERTIBLE SKETCHES IN MECHANICAL CURVED OBJECTS

A Malik sample sketch that includes many free-form curves [12] is shown in Fig. 5(a). In this figure, all line segments can be labeled uniquely, as shown in Fig. 5(b); thus, this sketch is theoretically realizable. However, it is obviously difficult to convert a sketch into a 3D model. First, it is impossible or wasteful to find SF(s) to handle a sketch because each SF is originally a primitive sketch familiar to humans, as shown in Fig. 1. Second, most people cannot imagine the 3D shape of a sketch precisely; therefore, the implementation of this conversion is unrealistic. Fig. 6 shows the nine SFs that we have found so far, except for the three SFs in Fig. 1. For example, polygonal extrusion is defined as a polygon and several parallelograms; each line segment of the polygon can become a line segment of a parallelogram, and two adjacent parallelograms share a line segment. The definitions of the other SFs are found in [21] and [23]. In Figs. 6(f) (g), and (h), the green lines indicate the cubic corners converted from the fillets. A detailed explanation of these SFs is provided in [18-21].

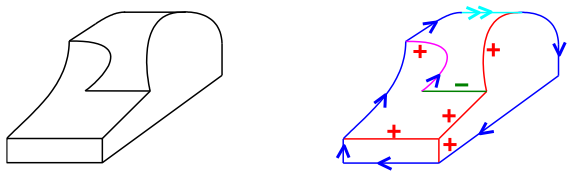

(a) (b)

Figure 5: Malik's sample sketch: (a) Sketch and (b) Line labelling.

(a) (b) (c) (d) (e) (f) (g) (h) (i)

Figure 6: Nine SFs: (a) Polygonal extrusion, (b) Multiple extrusion, (c) Rib, (d) Round rib, (e) Pipe, (f) Front fillet, (g) Side fillet, (h) Hidden fillet, and (i) Chain.

Consequently, convertible sketches can be limited when the objects are mechanical. To explore this limitation, we looked through the sketches of numerous mechanical objects, particularly curved objects, and identified the following tendencies:

- Cylindrical faces are typically drawn in sketches of mechanical curved objects. Toroidal and conical faces are sometimes drawn. Spherical faces are also occasionally drawn.
- Free-form curves are usually drawn in sketches of specialized machine covers, such as computer mice and car bodies, or fluid parts, such as electric fan blades. However, as shown in Fig. 5, the attempt to convert these sketches into 3D models is wasteful and/or unrealistic. Therefore, we excluded them from the convertible sketches in our study.
- Toroidal faces are typically drawn as fillets in mechanical objects. Conical faces are often drawn as the chamfers of cylindrical objects. Spherical faces are sometimes drawn as circles or arcs in sketches of rivets, caps, and nobs of levers.

These tendencies are illustrated in Figure 7. This figure shows sketches of the five types of cups with slightly different shapes. Fig. 7(a) shows a simple type that can be handled using SFBCM because it can be disassembled into a cylinder, round hole, and pipe sketch. Figs. 7(b) and 7(c) show the two curved cups. In Fig. 7(b), the two freeform curves contact an ellipse and an elliptical arc. Fig. 7(c) shows another curved type. Handling these is difficult using SFBCM because of the free-form curves. Fig. 7(d) shows a cup with a curved spout. Handling this using SFBCM is also difficult because of the definition of SF(s) of spout(s). Fig. 7(e) shows a conical type. If the SFs of a taper and tapered hole are defined, it is possible to handle them using SFBCM.

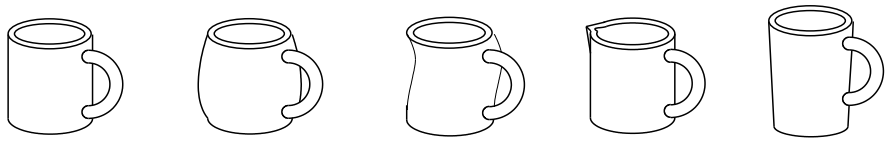

Figure 7: Sketches of four types of cups: (a) Simple, (b) Curved, (c) Another curved, (d) With a spout, and (e) Conical.

4 NEW SFS DEFINED FROM THE LIMITATION OF CONVERTIBLE SKETCHES

Several new SFs are defined based on the limitations of the aforementioned convertible sketches. Fig. 8 shows the six new SFs. Fig. 8(a) shows a concave flange consisting of two symmetrical arcs: a dotted ellipse and a dotted arc. These dotted lines are often invisible because they often become tangential to other SF(s). Fig. 8(b) shows a convex flange whose shape is the inverse of Fig. 8(a). These two SFs include sketches of toroidal faces. Fig. 8(c) shows a taper. Fig. 8(d) shows a tapered hole where an elliptical arc is not a part of an ellipse but is smaller. These two SFs include sketches of conical faces. Fig. 8(e) shows a tapered polygonal extrusion. Fig. 8(f) shows the tapered multiple extrusions.

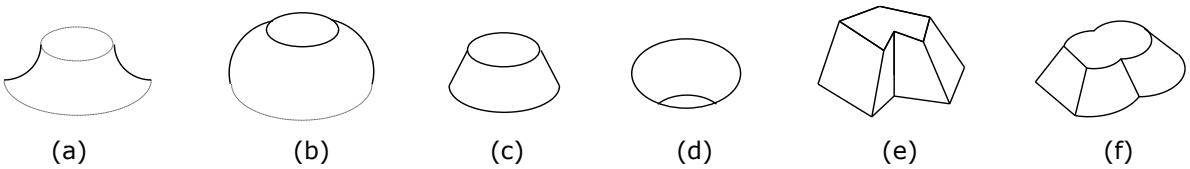

Figure 8: New six SFs: (a) Concave flange, (b) Convex flange, (c) Taper, (d) Tapered hole, (e) Tapered polygonal extrusion, and (f) Tapered multiple extrusion.

5 NEW ASFS OF SFS AND THE UPDATED ALGORITHM OF SFBCM

5.1 New ASFs of SFs

Each SFs in Fig. 8 can be partially hidden in sketches of mechanical curved objects. Introducing abstract sketch features (ASFs) into SFBCM can solve this problem. Each ASF is typically a straight-cut SF, as shown in Fig. 9. Fig. 9(a) shows a partial cuboid. Each isolated terminal of a line segment is marked with a blue point corresponding to a *T*-junction. Fig. 9(b) shows the two types of partial cylinders. Fig. 9(c) shows two types of partial polygonal extrusions. Fig. 9(d) shows two types of partial multiple extrusions. Fig. 9(e) shows the two types of partial ribs. Fig. 9(f) shows a partial pipe. Fig. 9(g) shows a partial chain. Fig. 9(h) and (i) show a partial spring and screw, respectively, although their SFs cannot be defined. All the ASFs in this figure are representative because there are many more types of ASFs. A more detailed explanation of the ASFs is provided in [18-19]. Fig. 10 shows the six ASFs shown in Fig. 8. In Fig. 10(d), we observe that an ellipse becomes an ASF of a round hole. Therefore, this ASF is called a partial round hole because cases of an ellipse corresponding to a tapered hole are rare. For ASF detection, two *Phantom-node*s can be effective.

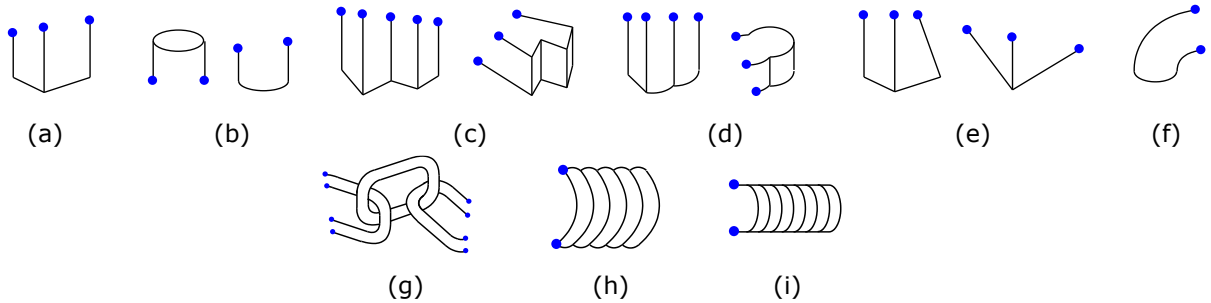

Figure 9: Nine ASFs: (a) Partial cuboid, (b) Two types of partial cylinders, (c) Two types of partial polygonal extrusions, (d) Two types of partial multiple extrusions, (e) Two types of partial ribs, (f) Partial pipe, (g) Partial chain, (h) Partial spring, and (i) Partial screw.

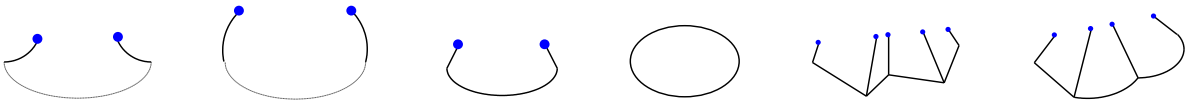

Figure 10: Six ASFs from Fig. 8: (a) Partial concave flange, (b) Partial convex flange, (c) Partial taper, (d) Partial round hole, (e) Partial tapered polygonal extrusion, and (f) Partial tapered multiple extrusion.

5.2 Updated Algorithm

Fig. 11 shows the algorithm of the updated SFBCM used in this study. Example 3 in Fig. 12(a) is Example 2 with a chain. This algorithm is explained in Example 3 as follows: In Step 1), all junctions are detected, as shown in Fig. 4(c), except for the chain. Most junctions in the chain are *T*-junctions. In Step 2), two ACSFs (ACSF1 and ACSF2) of the ring are detected, as shown in Fig. 12(b). In Step 4), a chain sketch (SF1) consisting of these components is detected, as shown in Fig. 12(c). In Step 7), SF1 is extracted as a 3D feature, as shown in Fig. 12(d). In Step 8), an isolated line segment that does not form any closed loops of lines is extended to the nearest line, and after performing Steps 1) to 3), a pipe sketch (SF2) is detected in Step 4). Subsequently, SF2 is extracted in Step 7), as shown in Fig. 12(e). In this figure, two isolated lines are connected (marked in light blue) in Step

8), and a multiple-extrusion sketch (SF3) is detected in Step 4). Next, the ASF of the round hole (ASF1) is detected in Step 5), as shown in Fig. 12(f). In Step 6), the length of ASF1 is predicted to fit the height of SF3, which becomes SF4, as shown in Fig. 12(g). Although SF4 can theoretically have a blind hole, this is rare in practice because of manufacturing difficulties. Step 7) extracts SF3 and SF4 as two 3D features. Next, a cuboid sketch (SF5) is detected in Step 4), as shown in Fig. 12(h) and then, the ASF of a cuboid (ASF2) is detected in Step 5), as shown in Fig. 12(i). In Step 6), ASF2 is predicted to contact the center of SF5 (detailed prediction methods are described in [19].) becoming SF6, as shown in Fig. 12(j). In Step 7), SF5 and SF6 are extracted as two 3D features. After this step, there are no lines; therefore, Steps 12), 13), and 14) are performed. Consequently, a 3D model is obtained, as shown in Fig. 12(k). Note that the steps not shown in this example are covered in other examples.

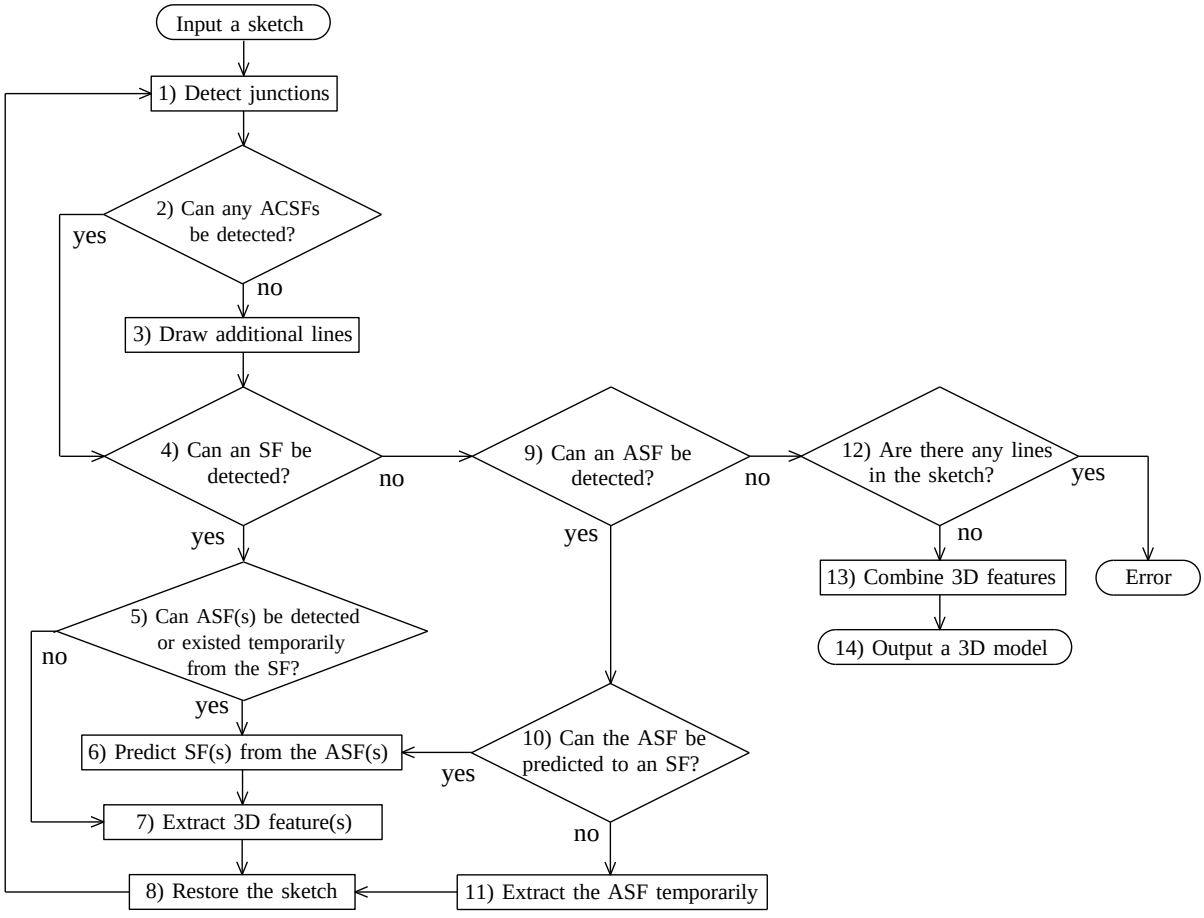

Figure 11: Updated SFBCM algorithm.

6 THREE ADVANCED EXAMPLES

6.1 Example 4

Fig. 13(a) shows Example 4, which is a sketch of the packing gland. When Example 4 is input into the updated SFBCM, first, the sketch of a tapered hole is detected, as shown in Fig. 13(b), because the elliptical arc is smaller in size than the ellipse.

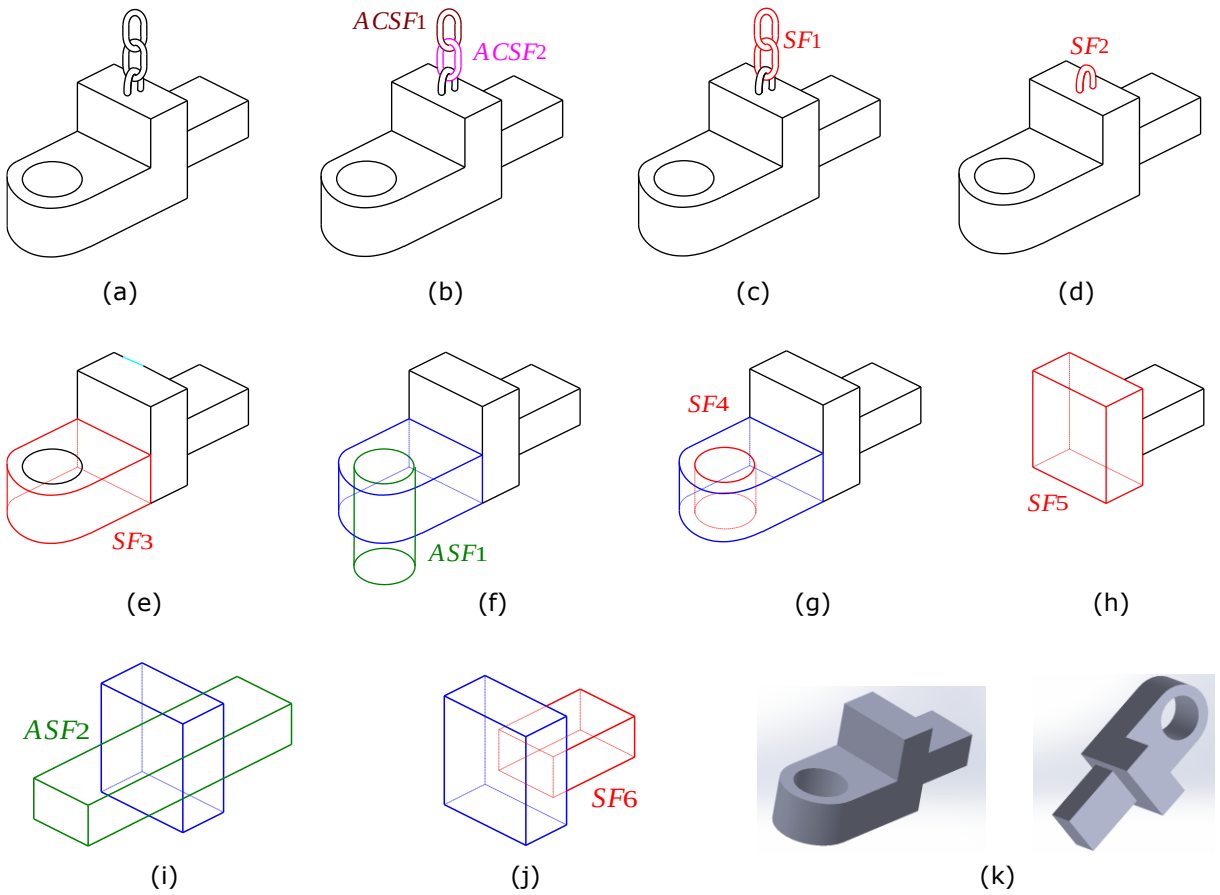

Figure 12: Updated SFBCM process (a) Example 3, (b) Two ACSFs of a ring, (c) SF1, (d) SF2, (e) SF3, (f) ASF1, (g) Prediction of ASF1 into SF4, (h) SF5, (i) ASF2, (j) Prediction of ASF2 into SF6, and (k) Two overviews of the solution.

Although a round hole should pass through the tapered hole, this case is discussed later. After 3D feature extraction, the ASF of the cylinder can be detected, as shown in Fig. 13(c). In this figure, the terminals of the two limb lines are indicated in blue. Each limb line is tangent to an arc and forms a *Curvature-L-junction*. The two green arcs are placed symmetrical to the cylinder so that they can form an SF or ASF of a flange. Consequently, a sketch of a cylinder sketch is predicted and detected, as shown in Fig. 13(d). After the 3D feature is extracted, two broken pink lines appear, as shown in Fig. 13(e). They can be connected by an extension, as shown in Fig. 13(f) although the shape of their connection does not match the solution of this example. Subsequently, a concave flange sketch is detected, as shown in Fig. 13(g). After the 3D feature is extracted, a multiple-extrusion sketch is detected, as shown in Fig. 13(h), and two ellipses are detected as two ASFs of round holes, as shown in Fig. 13(i). The depth of the holes is predicted to be the same as the height of the multiple-extrusion. Consequently, three 3D features are extracted, to obtain the solution for Example 4, as shown in Fig. 13(j). Fig. 13(k) shows the case in which a round hole passes through the tapered hole.

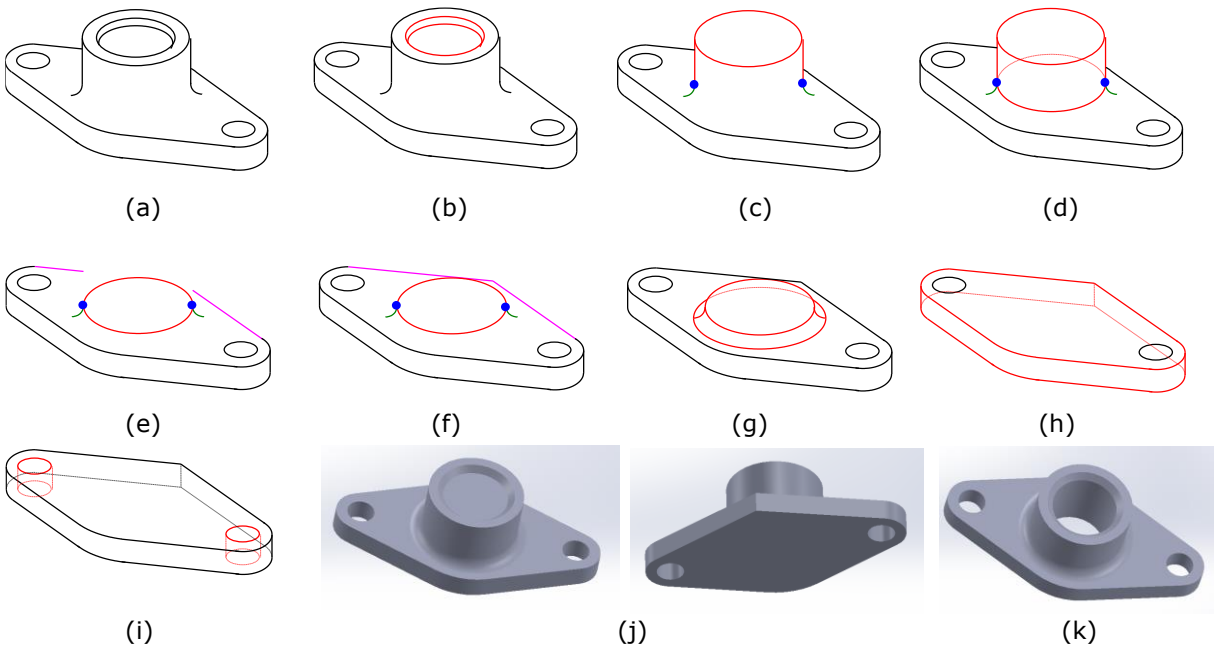

Figure 13: (a) Example 4, (b) Detection of a tapered hole, (c) Detection of a partial cylinder, (d) Prediction of a cylinder, (e) Extraction of the cylinder, (f) Restoration of two broken lines, (g) Detection of a concave flange, (h) Detection of a multiple extrusion, (i) Prediction of two round holes, (j) Two overviews of the solution, and (k) Addition of a round hole to (j).

6.2 Example 5

Fig. 14(a) shows Example 5, which is a sketch of the storage tank. Fig. 14(b) shows the three limb lines (green). Not drawing these would make it difficult for people to recognize the sketch. When this example is input into the updated SFBCM, first, the sketch of a cylinder is detected, as shown in Fig. 14(c). After extraction, the sketch of a convex flange is detected, as shown in Fig. 14(d). After the extraction of that, the ASF of a cylinder (green) is detected, as shown in Fig. 14(e), which is extracted temporarily, as shown in Fig. 14(f). These processes correspond to Steps 9), 10), and 11) in the updated algorithm. In this figure, the sketch of a cylinder (red) can be detected. Therefore, the length of the ASF can be predicted as the center of the detected cylinder (blue), as shown in Fig. 14(g). When these two SFs are extracted, a Bezier curve (green) remains. However, the curve cannot be ASFs; therefore, it is removed in Step 8) of the algorithm, whereby an ellipse and arc remain, as shown in Fig. 14(h). Handling these issues was difficult in the present study. Supposing that this figure shows the sketch of a hemisphere, the solution of Example 5 can be obtained as shown in Fig. 14(i).

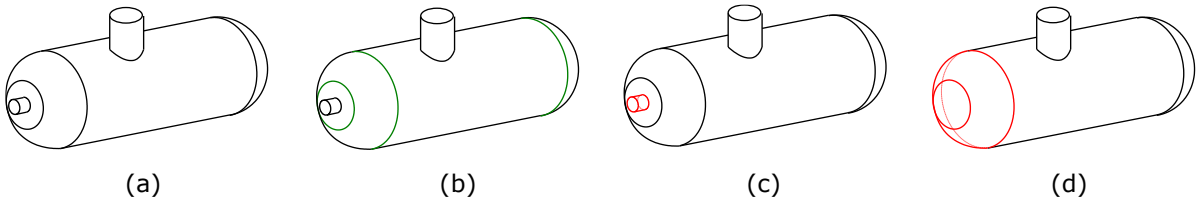

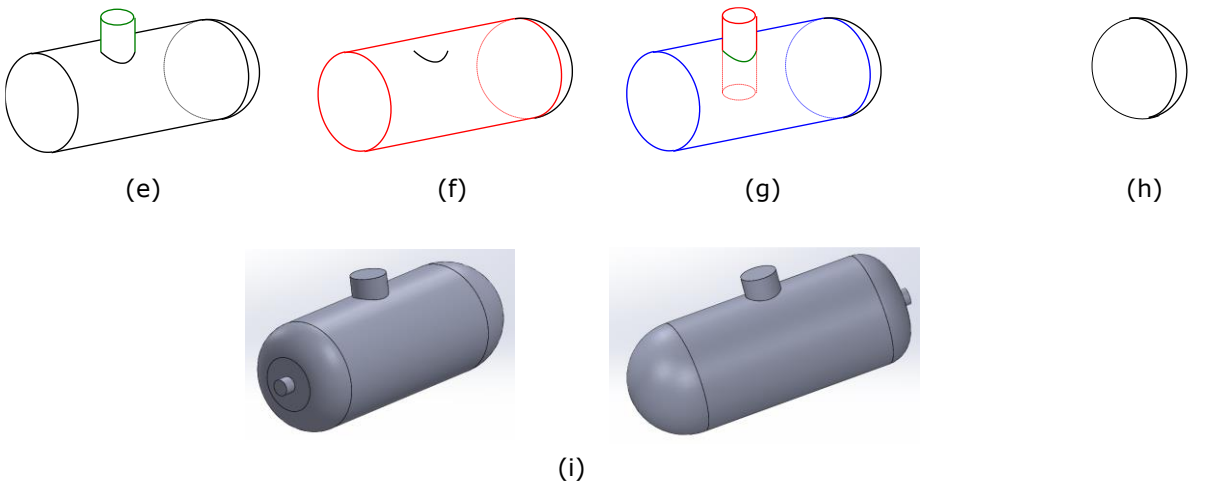

(e) (f) (g) (h)

(i)

Figure 14: (a) Example 5, (b) Three limb lines, (c) Detection of a cylinder, (d) Convex flange, (e) ASF of a cylinder, (f) Extraction of the ASF and detection of a cylinder sketch, (g) Prediction of ASF, (h) Remaining curved lines, and (i) Two overviews of the solution.

6.3 Example 6

Fig. 15(a) shows Example 6, which is a sketch of a multiport flange. When the sketch is input into the updated SFBCM, first, two ASFs of round holes are detected, as shown in Fig. 15(b). After extraction, two ASFs of cylinders are detected, as shown in Fig. 15(c). Similar to Example 4, two sketches of cylinders are detected, as shown in Fig. 15(d). From these sketches, the lengths of the two ASFs of the round holes are predicted to be the same as the lengths of the cylinders, as shown in Fig. 15(e). Two concave flange sketches are continuously detected, as shown in Fig. 15(f). Finally, the sketch of a cylinder is detected, as shown in Fig. 15(g). Consequently, a solution for Example 6 is obtained, as shown in Fig. 15(h). In Fig. 15(i), all its edges are displayed. In this figure, the two flanges do not overlap smoothly because the combination of 3D features is a simple addition. Therefore, considering smoothness when combining curved 3D features was an issue in our study.

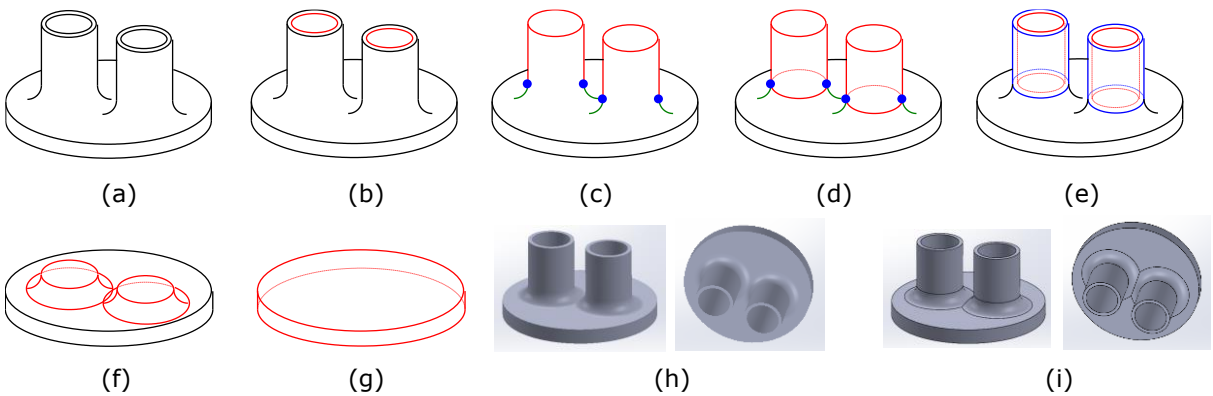

(a) (b) (c) (d) (e)

(f) (g) (h) (i)

Figure 15: (a) Example 6, (b) Two ASFs of round holes, (c) Two ASFs of cylinders, (d) Two cylinders, (e) Prediction of two round holes, (f) Detection of two concave flanges, (g) Detection of a cylinder, (h) Two overviews of the solution, and (i) Displayed all edges with (h).

7 DISCUSSION

In this study, we present 18 SFs, 15 ASFs, and two ACSFs. In practice, many more are required when dealing with more complex sketches of mechanical curved objects. Finding these was a constant challenge in this study. The sequence of detecting SFs, ASFs, and ACSFs is an important problem. In the algorithm shown in Fig. 11, ACSFs, SFs, and ASFs are detected in that order. The detection of ACSF(s) is the first step because the sketch of an ACSF is complex, unique, and symbolic. The detection of an SF is desirable next; however, there is a case in which an ASF prevents this detection. Therefore, Steps 9) to 11) extract that. In addition, a predicted ASF is extracted along with the SF to ensure that an ASF, such as an ellipse, does not float away from the input sketch during 3D feature extraction in Steps 5) to 7). This process corresponds to the CSG tree [14], in which two design or manufacturing features are combined step-by-step to create a mechanical object.

Additionally, the sequence of detecting and extracting SFs is an important issue. In many cases, SFBCM will output "Error" because of a mistake in the sequence. We found that this mistake was caused by the handling of additional lines. Therefore, drawing and using additional lines is important, especially in developing more practical conversion systems. In addition, simpler SFs are used prior to the other SFs in detection because they are more efficient to process. For example, cuboid sketches are detected before polygonal extrusion sketches. In practice, considering a more detailed sequence is challenging. Although we do not demonstrate our experimental system in this study because it is currently being developed, the 3D modeling platform for the implementation of SFBCM will be SimpleModeler, a product of Aikoku Alpha Corporation, a company two authors of this paper are associated with.

In this study, curved objects were more difficult to predict than polygonal objects. In Example 4, predicting whether the hidden corner is angular or round is difficult. Also, it is difficult for a human to visually determine whether a hole is tapered in Fig. 13(b). In addition, it is difficult to identify whether a hole has penetrated, as shown in Figs. 13(j) and (k). In Example 5, when the hidden part in Fig. 14(h) is predicted to be a sketch of a hemisphere, the solution is unbalanced, as shown in the right panel of Fig. 14(i). Solving these problems requires applying human perception and knowledge. Especially for mechanical objects, SFBCM is necessary, and machine-learning techniques may also be effective. In Example 6, dealing with the overlapping flanges was an issue, as previously described. The method for determining the ratio of the dimensions of a 3D model as the solution in each example, is based on the isometric conversion technique in SFBCM, as shown in Fig. 2(g). In this study, this decision was based on the *Y*-junction of the largest cuboid or the largest cylinder in the original sketch. However, whether a *Y*-junction or cylinder is suitable for the decision, or the course to adopt if there is no *Y*-junction or cylinder in the sketch, is still an issue.

Although this study clarifies the limitations of convertible sketches in mechanical curved objects, handling the sketches of numerous additional objects would be desirable. A hint is a simple sketch of organic objects that humans can easily recognize, such as animals and flowers. In particular, Entem et al. [8] presented a conversion method for organic objects, which is effective in inferring hidden shapes in sketches. Karpenko and Hughes [10] introduced SmoothSketch, which is a system for inferring plausible (but not precise) 3D free-form shapes from sketches. However, determining SFs from these is difficult. To address this issue from an engineering perspective, we contend that specializing in the conversion for each category would be more effective than generalizing it, especially for identifying unknown SFs.

8 CONCLUSIONS

In this study, convertible sketches of mechanical curved objects into 3D models were clarified using five examples. The results of this study can be summarized as follows.

- Although a sketch is theoretically realizable when all its lines are uniquely labeled, sketches including many free-form curves are difficult to convert into 3D models. Therefore, they were excluded from convertible sketches in SFBCM.

- Six new SFs and their ASFs were defined for handling sketches of conical and toroidal faces, which are often used in mechanical curved objects. For this purpose, the SFBCM algorithm was updated, particularly the detection sequence.
- The effectiveness and several issues of the updated SFBCM are indicated and discussed through examples. Moreover, the effectiveness of the isometric conversion technique in SFBCM is presented in all the presented examples.

Masaji Tanaka, https://orcid.org/0000-0002-5266-9182

REFERENCES

[1] Alhamazani, F.; Lai, Yu-Kun; Robin, Paul L.: 3DCascade-GAN: Shape completion from single-view depth images, Computers & Graphics, 115, 2023, 412-422, https://doi.org/10.1016/j.cag.2023.07.033

[2] Biederman, I: Recognition-by-components: a theory of human image understanding, Psychological Review, 94(2), 1987, 115-147, https://doi.org/10.1037/0033-295X.94.2.115

[3] Biederman, I: Recognizing depth-rotated objects: a review of recent research and theory, Spatial Vision, 13, 2001, 241-253, https://doi.org/10.1163/156856800741063

[4] Camba, J. D.; Company, P.; Naya, F.: Sketch-Based Modeling in Mechanical Engineering Design: Current Status and Opportunities, Computer-Aided Design, 150, September 2022, 103283, https://doi.org/10.1016/j.cad.2022.103283

[5] Chen, S.; Shao, D.; Zhang, L.; Zhang, C.: Learning depth-aware features for indoor scene understanding, Multimedia Tools and Applications, 81, 2022, 42573–42590, https://doi.org/10.1007/s11042-021-11453-3

[6] Clowes, M.B.: On seeing things, Artificial Intelligence, 2(1), 1971, 79–116, https://doi.org/10.1016/0004-3702(71)90005-1

[7] Company, P.; Piquer, A.; Contero, M.; Naya, F.: A survey on geometrical reconstruction as a core technology to sketch-based modeling, Computers & Graphics, 29(6), 2005, 892–904, http://dx.doi.org/10.1016/j.cag.2005.09.007

[8] Entem, E.; Parakkat, A. D.; Barthe, L.; Muthuganapathy, R.; Cani, M.-P.: Automatic structuring of organic shapes from a single drawing, Computers & Graphics, 81, 2019, 125-139, https://doi.org/10.1016/j.cag.2019.04.006

[9] Huffman, D. A.: Impossible objects as nonsense sentences, Machine Intelligence 6, 1971, 295–323.

[10] Karpenko, O. A.; Hughes, J. F.: SmoothSketch: 3D free-form shapes from complex sketches, ACM Transactions on Graphics, 25(3), 2006, 589-598, https://doi.org/10.1145/1141911.1141928

[11] Kirousis, L. M.; Papadimitriou, C. H.: The complexity of recognizing polyhedral scenes, Journal of Computer System Sciences, 37(1), 1988, 14–38, http://dx.doi.org/10.1016/0022-0000(88)90043-8

[12] Malik, J.: Interpreting line drawings of curved objects, International Journal of Computer Vision, 1, 1987, 73–103. http://dx.doi.org/10.1007/BF00128527

[13] Perkins, D. N.: Cubic Corners, Quarterly Progress Report 89, MIT Research Laboratory of Electronics, 1968, 207–214.

[14] Plumed, R.; Company, P.; Varley, P. A. C.; Martin, R. R.: CSG Feature Trees from Engineering Sketches of Polyhedral Shapes, EUROGRAPHICS 2014, https://doi.org/10.2312/egsh.20141008

[15] Ren, H.; El-khamy, M.; Lee, J.: Deep Robust Single Image Depth Estimation Neural Network Using Scene Understanding, arXiv:1906.03279, 2019, https://doi.org/10.48550/arXiv.1906.03279

[16] Suh, Y. S.: Reconstructing Polyhedral CAD Models by Recognizing Extrusion Features from Single-View Drawings, ASME 2007 International Design Engineering Technical Conferences and

Computers and Information in Engineering Conference, DETC2007-35186, 2007, 197-206, https://doi.org/10.1115/DETC2007-35186
[17] Suh, Y. S.: Reconstructing Polyhedral Swept Volumes from a Single-View Sketch, 2006 IEEE International Conference on Information Reuse & Integration, 2006, https://doi.org/10.1109/IRI.2006.252479
[18] Tanaka, M.; Asano, T.; Higashino, C.; Ohtsuki, M.: Handling Chains, Springs, and Screws for Automatic Conversion of Mechanical Sketches into 3D Models, Computer-Aided Design & Applications, 21(1), 2024, 29-38, https://doi.org/10.14733/cadaps.2024.29-38
[19] Tanaka, M.; Asano, T.; Higashino, C.: Abstraction of Sketch Features for Predicting Hidden Shapes of Sketches for The Automatic Conversion into 3D Models, Computer-Aided Design & Applications, 19(5), 2022, 977-987, https://doi.org/10.14733/cadaps.2022.977-987
[20] Tanaka, M.; Asano, T.; Higashino, C.: Isometric Conversion of Mechanical Sketches into 3D Models, Computer-Aided Design & Applications, 18(4), 2021, 772-785, https://doi.org/10.14733/cadaps.2021.772-785
[21] Tanaka, M.; Terano, M.; Asano, T.; Higashino, C.: Method to Automatically Convert Sketches of Mechanical Objects into 3D Models, Computer-Aided Design & Applications, 17(6), 2020, 1168-1176, https://doi.org/10.14733/cadaps.2020.1168-1176
[22] Tanaka, M.; Terano, M.; Higashino, C.; Asano, T.; Takasugi, K.: A Learning Method for Reconstructing 3D Models from Sketches, Computer-Aided Design & Applications, 16(6), 2019, 1158-1170, https://doi.org/10.14733/cadaps.2019.1158-1170
[23] Tanaka, M.; Kaneeda, T.: Feature extraction from sketches of objects, Computer-Aided Design & Applications, 12(3), 2014, 300-309. http://dx.doi.org/10.1080/16864360.2014. 981459
[24] Varley, P. A. C.; Martin, R. R.; Suzuki, H.: Frontal geometry from sketches of engineering objects: is line labelling necessary?, Computer-Aided Design, 37(12), 2005, 1285–1307, https://doi.org/10.1016/j.cad.2005.01.002
[25] Yang, B.; Wen, H.; Wang, S.; Clark, R.; Markham, A.; Trigoni, N.: 3D Object Reconstruction from a Single Depth View with Adversarial Learning, arXiv:1708.07969, 2017, https://doi.org/10.48550/arXiv.1708.07969